

A Variable Structure Controller for a Class of Hyper-redundant Arms

Decebal Popescu¹, Nirvana Popescu¹, Mircea Ivanescu² and Dorin Popescu²

¹Department of Computing Science, POLITEHNICA University of Bucharest, Splaiul Independentei, Bucharest, Romania

²Department of Mechatronics, University of Craiova, A.I. Cuza, Craiova, Romania

Keywords: Hyper-redundant Robot, Continuum Arms, Control.

Abstract: The paper treats the control problem of a class of hyper-redundant robot constituted by a chain of continuum segments. The technological model basis is a central, long and thin, highly flexible and elastic backbone. The driving system is a decoupled one. The main parameters of the arm control are determined by the curvature and curvature gradient. The dynamic model is inferred. A sliding mode control system is used in order to achieve a desired shape of the arm. The stability of the closed loop control system is proven. Numerical simulations are also provided to verify the effectiveness of the presented approach.

1 INTRODUCTION

The goal of this paper is to implement a control system for a class of hyper-redundant robots with continuum components. The tentacle robots represent one of the most attractive domains of robotics during the last decades. The control of these systems is very complex and several researchers have tried to offer solutions as it will be further discussed. In (Chirikjian, 1990), (Robinson, 1999), (Gravagne, 2000), (Gravagne and Walker, 2000), (Jones and Walker, 2006) the kinematic models were analysed, based on a “backbone curve” that captures the robot’s macroscopic geometric features. In (Mochiyama, 1999), (Hirose and Umetani, 1976) the problem of controlling the shape of a robot with two-degree-of-freedom joints was also investigated using spatial curves. A controller for continuum robots was developed by using neural network feed-forward components in (Braganza, 2007). Other researchers derived a new kinematic model by using the differential geometry (Walker, 1999), (Kapadia, Walker and Dawson, 2009), (Hannan, 2005) or introduced a real-time controller for continuum robots (Jones, 2006). In (Kapadia, 2009) it was proposed a sliding controller for extensible robots. Other papers (La Spina, 2007), (KeJun, 2009), (Webster and Jones, 2010) have developed several biomimetic prototypes with undulatory action.

Our paper treats the control problem of a class of light weight hyper-redundant robots. The

technological model basis is a central, long and thin, highly flexible and elastic backbone. The driving system is a decoupled one. The main parameters of the arm control are determined by the curvature and curvature gradient. The dynamic model is inferred. A sliding mode control system is used in order to achieve a desired shape of the arm.

The paper is structured as follows: section 2 presents technological structure, section 3 analyses the dynamic model, section 4 treats the control algorithm, section 5 verifies the control laws by computer simulation and section 6 contains the conclusions.

2 TECHNOLOGICAL ARM

The technological model basis is an arm with a distributed mass. The 3D model basis from Fig 1 consists of a central, long and thin, highly flexible and elastic backbone. It is made from homogeneous materials, the bending represents the main motion and we neglect the deformations of axial tension/compression and shear. The arm is divided in several segments, each segment having its own driving system. The motion of the arm, the bending, is determined by antagonistic cables (tendons) attached to the terminal point of each segment and a DC motor driving system. These cables develop the driven torques τ_i , $i=1, 2, \dots$

The cables ensure an independent bending for each segment so that the segment driving control is a decoupled one.

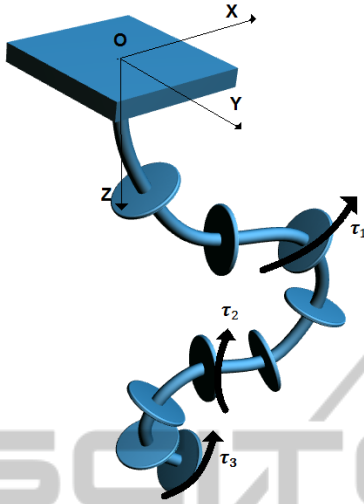


Figure 1: The technological arm.

3 DYNAMIC MODEL

We consider a hyper-redundant arm constituted by a serial connection of a number of continuum arm segments, with equal lengths L (Fig 2). For the segment i , the curvature is defined by

$$\kappa_{0i}(0) = \frac{d\omega^i(s=0)}{ds} = \left[\frac{d\theta^i(s=0)}{ds} \right] \left[\frac{dq^i(s=0)}{ds} \right] \quad (1)$$

$$\kappa_{1i}(L) = \frac{d\omega^i(s=L)}{ds} = \left[\frac{d\theta^i(s=L)}{ds} \right] \left[\frac{dq^i(s=L)}{ds} \right]$$

and we assume that the continuity of the arm curvature requires the following segment boundary conditions

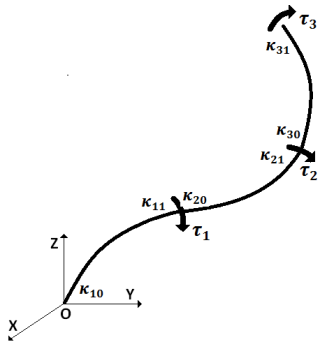


Figure 2: The backbone model.

$$\kappa_{0i}(0) = \kappa_{1i-1}(L) \quad (2)$$

with

$$\kappa_{00}(0) = 0 \quad (3)$$

Using the same procedure as in (Gravagne, 2000), we obtain the partial differential equations (PDE) of the arm segment,

$$I_p \ddot{\omega}^i = EI \omega_{ss}^i - B \dot{\omega}^i + h^i(\omega^i) \quad (4)$$

where $\omega^i = \omega^i(t,s)$, $\omega^i = (\theta^i, q^i)^T$, $s \in \Omega$, $\dot{\omega}^i = \partial\omega^i/\partial t$, $\omega_s = \partial\omega^i/\partial s$, I_p is the rotational inertial density matrix, $I_p = \text{diag}(I_{p\theta}, I_{pq})$, $I_{p\theta} = I_{pq} = I_p$, B is the equivalent damping matrix of the arm, $B = \text{diag}(b_\theta, b_q)$, $b_\theta = b_q = b$ and h represents the nonlinear component vector determined by gravitational components, $h^i = (h_1^i, h_2^i)^T$. The initial and boundary conditions are

$$\omega^i(0,s) = \omega_0^i(s) \quad (5)$$

$$EI \omega_s^i(t,l) = \tau_i(t), \quad \omega_s^i(t,0) = 0 \quad (6)$$

$$\omega_s^0(t,0) = 0 \quad (7)$$

$$\omega^0(t,0) = 0 \quad (8)$$

where τ_i is the equivalent moment generated by the forces F_i at the end of the arm segment i , $\tau_i(t) = F_i \cdot r$, r is the radix of the moment,

$$\tau_i = \begin{bmatrix} \tau_{\theta i} \\ \tau_{q i} \end{bmatrix}, \quad F_i = \begin{bmatrix} F_{\theta i} \\ F_{q i} \end{bmatrix} \quad (9)$$

The dynamic model of the arm can be expressed in terms of the curvature $\kappa_{1i}(t,L)$ as

$$I_p \frac{L}{2} A \ddot{\kappa}(t) = -b \frac{L}{2} A \dot{\kappa}(t) - \frac{EI}{L} C \kappa(t) + \frac{1}{L} \tau(t) + h(\kappa) \quad (10)$$

$$\kappa(0) = \kappa_0 \quad (11)$$

where

$$\kappa = (\kappa_{11}, \kappa_{12}, \dots, \kappa_{1n})^T \quad (12)$$

with

$$\kappa_i(t) = \kappa_{1i}(t, L) \quad (13)$$

represents the new state vector, $\kappa \in R^n$, τ denotes the general input of the arm,

$$\tau = (\tau_1, \tau_2, \dots, \tau_n)^T \quad (14)$$

the linear components are defined by the $(n \times n)$ matrices

$$A = \begin{bmatrix} 1 & 0 & 0 & 0 & \dots & 0 \\ 2 & 1 & 0 & 0 & \dots & 0 \\ 2 & 2 & 1 & 0 & \dots & 0 \\ \dots & \dots & \dots & \dots & \dots & \dots \\ 2 & 2 & 2 & 2 & 2 & 1 \end{bmatrix}, \quad C = \begin{bmatrix} 0 & 0 & 0 & \dots & 0 \\ 1 & 0 & 0 & \dots & 0 \\ 0 & 1 & 0 & \dots & 0 \\ \dots & \dots & \dots & \dots & \dots \\ 0 & 0 & 0 & \dots & 1 & 0 \end{bmatrix} \quad (15)$$

and the nonlinear component is determined by

$$h=(h^1,h^2,\dots,h^n)^T \quad (16)$$

where $h^i = h^i(\kappa_i)$ and satisfies the inequality (Popesu,2014)

$$\|h(\omega)\| \leq M \|\kappa\| \quad (17)$$

4 CONTROL ALGORITHM

We consider a desired state $\kappa^d, \kappa^d \in \mathbb{R}^n$, that satisfies (10) with initial condition (11) and we define by

$$e(t) = \kappa^d - \kappa(t) \quad (18)$$

the error variable, $e \in \mathbb{R}^n$.

The control problem consists of finding the control law $\tau(t)$, on the boundary $s=L$ of each segment such that the error converges to zero.

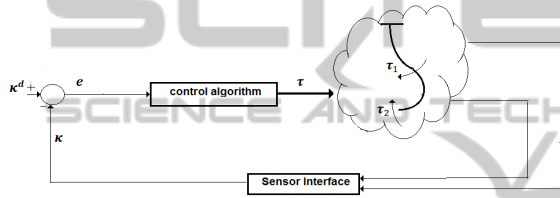


Figure 3: The control system.

The main idea of the control system is based on the variable structure control associated with the special properties of the physical system. We propose a controller with a boundary torque variable structure control. Let us define by $S(t)$ the sliding surface, associated with the model (10) and the error (18)

$$S(t) = e(t) + \sigma \dot{e}(t) \quad (19)$$

where $S = (S_1, S_2, \dots, S_n)^T$, $\sigma = \text{diag}(\sigma_1, \sigma_2, \dots, \sigma_n)$, σ_i are positive constants.

Theorem 1. For the system described by (10) with the initial conditions (11), if the variable structure controller is given by

$$\Delta \tau = -K_1 \text{sgn}(S) - K_2 C e \text{sgn}(S^T K_2 C e) \quad (20)$$

$$-K_3 A (I_p \sigma^{-1} - b I) \dot{e} \text{sgn}(S^T A (I_p \sigma^{-1} - b I) \dot{e}) \quad (21)$$

$$K_1 > 0 \quad (22)$$

$$K_2 C - M I - \frac{EI}{L} C > 0 \quad (22)$$

$$\left(\frac{K_3}{L} - \frac{L}{2} I \right) (I_p A \sigma^{-1} - b I) > 0 \quad (23)$$

where $K_j = \text{diag}(k_{j1}, k_{j2}, \dots, k_{jn})$, $j=1, 2, 3$ represent

the control coefficients, then the motion of the system will reach the sliding line $S=0$ and then keep it there, where $\Delta \tau$ is defined by

$$\tau = \tau^d - \Delta \tau \quad (24)$$

and τ^d represents the torque vector on the desired position κ^d that satisfies the equations,

$$-\frac{EI}{L} C \kappa^d + \frac{1}{L} \tau^d + h(\kappa^d) = 0 \quad (25)$$

Proof. See Appendix

5 NUMERICAL SIMULATIONS

Consider a dynamic model of a vertical hyper-redundant arm, with two arm segments, with the length of the segment $L=1$ m, the rotational inertial density $I_p = 0.001$ kg m^2 , the bending stiffness $EI = 0.1$ Nm 3 , the viscous coefficient $b_\theta = 0.06$ Nms/rad. These constants are scaled to realistic ratios for a long thin arm. The initial and boundary conditions are: $\theta_0(s) = 0$, $\theta_s(t, 0) = 0$, $EI \theta_s(t, L) = \tau$, where τ is the torque applied at the top of the arm segment. We consider that the uncertain term $h(\theta)$ is defined by the gravitational components. For the characteristic values of the arm parameters, $\rho_b = 0.8$ kg/m, $g = 10$ m/s 2 , $A = 4 \cdot 10^{-4}$ m 2 , associated with this thin long arm, the inequality (17) is satisfied for $M = 10$. The arm is simulated by a chain of vertebrae.

We simulated two motions. The first motion is a XOZ plan motion, the arm (the both segments) is moving toward the desired position defined in term of curvature, $\kappa_{\theta d} = -\frac{\pi}{14}$. A control law (20) with the controller gains, $k_{1\theta}^i = 20$, $k_{2\theta}^i = 8$, $k_{3\theta}^i = 3$ is used, where $k_{1\theta}^i, k_{2\theta}^i, k_{3\theta}^i, i=1, 2, \dots$, verifies the conditions (21) - (23). The motion of the arm, several intermediary positions and final positions are illustrated in Figure 4.

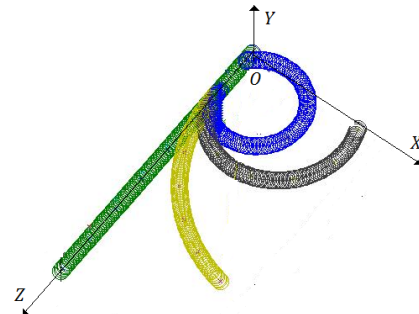


Figure 4: A XOZ plan motion.

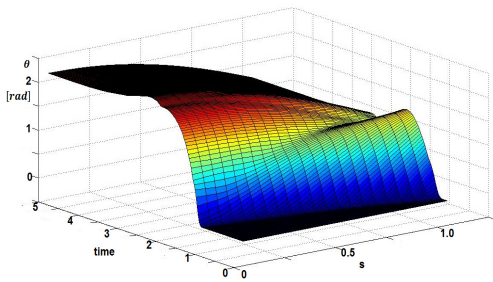


Figure 5: The state evolution for the plan motion.

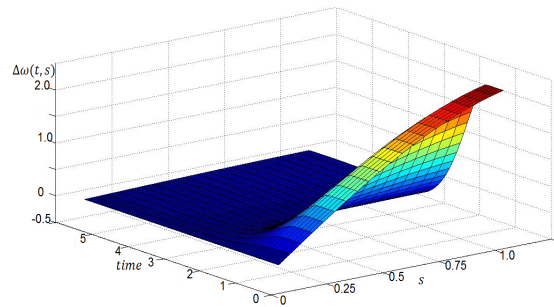


Figure 7: The error evolution for the 3D motion.

The time evolution can be analysed if we use the distributed parameter dynamic model described by PDE (4) with boundary conditions defined by the control law of torque (20). The state variable evolution is presented in Fig 5.

A 3D motion of a 2-segment arm is presented in Figure 6. The desired position is defined by $\kappa_{10d} = \kappa_{20d} = -\pi/14$, $\kappa_{1qd} = \kappa_{2qd} = -\pi/24$. The control parameters were selected as $k_{10}^i = k_{1q}^i = 20$, $k_{20}^i = k_{2q}^i = 8$, $k_{30}^i = k_{3q}^i = 3$, $i = 1, 2, \dots$. The both segments bend with the same curvature. The error evolution is presented in Figure 7. In Figure 8 is presented a new motion of this arm, with a different desired position of each arm segment:

$$\kappa_{10d} = -\pi/14, \kappa_{1qd} = -\pi/24, \kappa_{20d} = \pi/14, \kappa_{2qd} = -\pi/24$$

The good performances of the proposed control algorithm are concluded from the graphics.

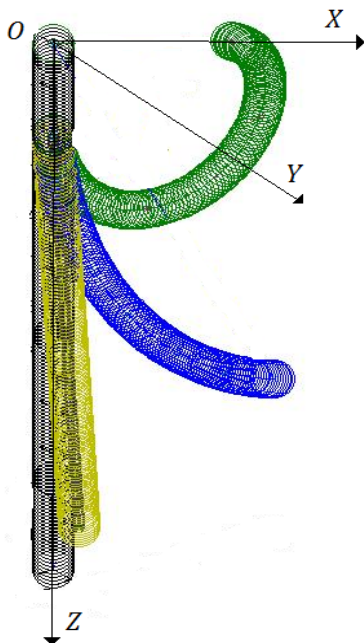


Figure 6: A 3D motion: $\kappa_{10d} = \kappa_{20d} = -\frac{\pi}{14}$, $\kappa_{1qd} = \kappa_{2qd} = -\frac{\pi}{24}$.

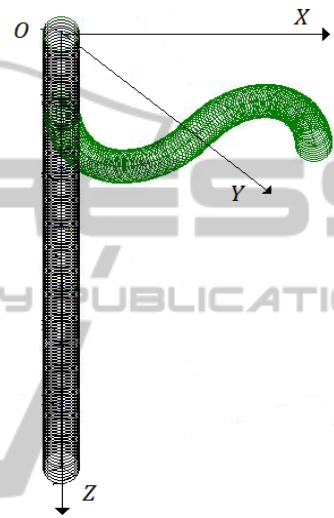


Figure 8: A 3D motion $\kappa_{10d} = -\frac{\pi}{14}$, $\kappa_{1qd} = -\frac{\pi}{64}$, $\kappa_{20d} = \frac{\pi}{14}$, $\kappa_{2qd} = -\frac{\pi}{64}$.

6 CONCLUSIONS

The paper presents the control problem of a class of hyper-redundant robot constituted by a chain of continuum segments. The technological model basis is a central, long and thin, highly flexible and elastic backbone. The driving system is a decoupled one. The main parameters of the arm control are determined by the curvature and curvature gradient. The dynamic model is inferred in terms of the curvature. A sliding mode control system is used in order to achieve a desired shape of the arm. The stability of the closed loop control system is proven. Numerical simulations are also provided to verify the effectiveness of the presented approach.

ACKNOWLEDGEMENTS

This work has been supported by PPCA 150/2012 grant of the Romanian Executive Agency for Higher Education, Research, Development and Innovation Funding (UEFISCDI).

REFERENCES

Robinson, G., Davies, G. B. C., 1999 “Continuum Robots – a State of the Art”, *Proc. IEEE Int. Conf. on Robotics and Automation*, Detroit, May 1999, Pp. 2849 – 2854.

Gravagne, Ian A., Walker, Ian D., 2000, on the Kinematics of Remotely - Actuated Continuum Robots, *Proc. 2000 IEEE Int. Conf. on Robotics and Automation*, San Francisco, April 2000, Pp. 2544-2550.

Gravagne, Ian A., Walker, Ian D., Kinematic Transformations for Remotely-Actuated Planar Continuum Robots, *Proc. 2000 IEEE Int. Conf. on Rob. and Aut.*, San Francisco, April 2000, Pp. 19-26.

Chirikjian, G. S., Burdick, J. W., 1990, an Obstacle Avoidance Algorithm for Hyper-Redundant Manipulators, *Proc. IEEE Int. Conf. on Robotics and Automation*, Cincinnati, Ohio, May 1990, Pp. 625 – 631.

Mochiyama, H., Kobayashi, H. 1999, the Shape Jacobian of a Manipulator with Hyper Degrees of Freedom, *Proc. 1999 IEEE Int. Conf. on Robotics and Automation*, Detroit, May 1999, Pp. 2837- 2842.

Braganza, D., D.M. Dawson, Walker, N. Nath, N., 2007, “A Neural Network Controller for Continuum Robots”, *IEEE Transaction Robotics*, Vol. 23, Issue 6, Dec. 2007, Pp. 1270 – 1277.

Walker, I., M. Hannan, M., 1999, “A Novel Elephant’s Trunk Robot”, *AIM ’99*, Pp. 410 – 415.

Jones, B., I. D. Walker, 2006, “Practical Kinematics for Real-Time Implementation of Continuum Robots”, *IEEE Trans. Robotics*, Vol. 22, No. 6, Dec. 2006, Pp. 1087 – 1099.

Kapadia, I. Walker, D. Dawson, 2009 “a Model – based Sliding Mode Controller for Extensible Continuum Robots”, *Recent Advances in Signal Processing, Robotics and Automation*, ISPRA Conf., 2009, Pp. 103 – 120.

Popescu, N., Popescu, D., Ivanescu, M., Nitulescu, M., 2014, the Curvature Control of a Hyper-Redundant Robot *Proc. of Int. Symp of Robotics*, Munich, June, 2014, Pp 251-257.

G. La Spina, M. Sfakiotakis, D. Tsakiris, a. Memciassi, P. Dario, 2007, Polychaete-like Undulatory Robotic Locomotion in Unstructured Substrates, *IEEE Trans on Robotics*, Vol 23, No 6, Febr 2007, Pp 1200-1212.

Kejun Ning, F. Worgotter, 2009, a Novel Concept for Building a Hyper-Redundant Chain Robot, *IEEE Trans on Robotics*, Vol 25, No 6, Dec 2009, Pp 1237-1248.

Rucker, D. C., B. A. Jones, R. J. Webster III, 2010, a Geometrically Exact Model for Externally Loaded Concentric-Tube Continuum Robots, *IEEE Trans on Robotics*, Vol 26, No 5, Oct 2010, Pp 769-780.

Bailly, Y., Y. Amirat, G. Fried, Modeling and Control of a Continuum Style Microrobot for Endovascular Surgery, *IEEE Trans on Robotics*, Vol 27, No 5, Oct 2011, Pp 1024-1030.

Bajo, A., N. Simaan, 2012, Kinematics-based Detection and Localization of Contacts along Multisegment Continuum Robots, *IEEE Trans on Robotics*, Vol 28, No 2, April 2012, Pp 291-302.

B. A. Jones, I. D. Walker, „Kinematics for Multisection Continuum Robots”, *IEEE Transactions on Robotics*, VOL. 22, NO. 1, Febr. 2006, 43- 51.

R. Fareh, M. Saad, M. Saad, „Workspace Tracking Trajectory for 7-DOF ANAT Robot using a Hierarchical Control Strategy”, *2012 20th mediterranean Conference on Control & Automation (MED)*, Barcelona, Spain, July 3-6, 2012 122-128.

H. Shang, J. F. Forbes, and M. Guay. “Feedback Control of Hyperbolic Distributed Parameter Systems”, *Chemical Engineering Science*, 60:969 – 980, 2005.

F. Fahimi, H. Ashrafiuon, and C. Nataraj, (2002) “an Improved Inverse Kinematic and Velocity Solution for Spatial Hyper-Redundant Robots,” *IEEE Trans. on Robotics and Automation*, Vol. 18, No. 1, Feb. 2002, Pp. 103–107.

S. Hirose, Umetani, Y., (1976), Kinematic Control of Active Cord Mechanism with Tactile Sensors, *Proc of 2nd Int CISM-IFT Symp. on Theory and Practice of Robots and Manipulators*, Pp 241-252, 1976.

A. Kapadia, I. Walker, D. Dawson, (2009), “a Model – based Sliding Mode Controller for Extensible Continuum Robots”, *Recent Advances in Signal Processing, Robotics and Automation*, ISPRA Conf., 2009, Pp. 103 – 120.

R. J. Webster, B. A. Jones, “Design and Kinematic Modelling of Constant Curvature Continuum Robots: a Review”, *the International Journal of Robotics Research*, 29 (13), 2010, Pp. 1661-1683,

M. W. Hannan, “Real-Time Estimation for Continuum Robots using Vision”, *Robotica*, Vol 23 /Issue 05, Sept. 2005, Pp 645-661.

APPENDIX

From (10) - (11), the error dynamics will be described by

$$I_p \frac{L}{2} A \ddot{\mathbf{e}}(t) = -b \frac{L}{2} A \dot{\mathbf{e}}(t) - \frac{EI}{L} C \mathbf{e}(t) + \frac{1}{L} \Delta \boldsymbol{\tau}(t) + \Delta \mathbf{h}(\boldsymbol{\kappa}^d) \quad (\text{A.1})$$

$$\mathbf{e}(0) = \mathbf{e}_0 \quad (\text{A.2})$$

$$\Delta \mathbf{h} = \mathbf{h} - \mathbf{h}(\boldsymbol{\kappa}^d) \quad (\text{A.3})$$

Let us consider the Liapunov function

$$V(t) = \frac{1}{4} \mathbf{1}^T \mathbf{S}^T(t) \mathbf{I}_p \mathbf{A} \sigma^{-1} \mathbf{S}(t) \quad (\text{A.4})$$

The time derivative of $V(t)$ is given by

$$\dot{V} = \frac{1}{2} \mathbf{S}^T \mathbf{I}_p \mathbf{A} \sigma^{-1} \dot{\mathbf{S}} \quad (\text{A.5})$$

where in order to simplify the notation, the variable t is omitted.

$$\dot{V} = \frac{1}{2} \mathbf{S}^T \mathbf{I}_p \mathbf{A} \sigma^{-1} (\dot{\mathbf{e}} + \sigma \ddot{\mathbf{e}}) \quad (\text{A.6})$$

By evaluating (A.6) along with the solutions of (A.1), it turns out that

$$\begin{aligned} \dot{V} = & \frac{L}{2} \mathbf{S}^T (\mathbf{I}_p \mathbf{A} \sigma^{-1} - \mathbf{A} \mathbf{b}) \dot{\mathbf{e}} - \frac{EI}{L} \mathbf{S}^T \mathbf{C} \mathbf{e} + \mathbf{S}^T \Delta \mathbf{h} \\ & + \frac{1}{L} \mathbf{S}^T \Delta \boldsymbol{\tau} \end{aligned} \quad (\text{A.7})$$

Now, substituting the control $\Delta \boldsymbol{\tau}$ from (20), after simple additional manipulations, we obtain

$$\begin{aligned} \dot{V} \leq & -\frac{1}{L} K_1 \|S\| - \|\mathbf{S}^T\| \left(K_2 \mathbf{C} - \mathbf{M} \mathbf{I} - \frac{EI}{L} \mathbf{C} \right) \|\mathbf{e}\| \\ & - \|\mathbf{S}^T\| \left(\frac{K_3}{L} - \frac{L}{2} \mathbf{I} \right) (\mathbf{I}_p \mathbf{A} \sigma^{-1} - \mathbf{b} \mathbf{I}) \|\dot{\mathbf{e}}\| \end{aligned} \quad (\text{A.8})$$

Using the conditions (21) - (23), this inequality can be rewritten as

$$\dot{V} \leq -\frac{1}{L} K_1 \|S\| \quad (\text{A.8})$$